PREDICTING SPALL AND BREACH FOR BLAST-LOADED REINFORCED-CONCRETE COLUMNS

John M. H. Puryear, PE, Protection Engineering Consultants, Austin, TX, USA
David J. Stevens, PhD, PE, Protection Engineering Consultants, San Antonio, TX, USA
Kirk A. Marchand, PE, Protection Engineering Consultants, San Antonio, TX, USA
Eric B. Williamson, PhD, PE, University of Texas, Austin, TX, USA
Eric L. Sammarco, PE, University of Texas, Austin, TX, USA
C. Kennan Crane, PhD, PE, US Army Engineer Research and Development Center, Vicksburg, MS, USA

ABSTRACT

Reinforced concrete (RC) elements subjected to a close-in detonation may spall or breach. Spall refers to the loss of cross section through part of an element's thickness; breach refers to the loss of cross section through the entire thickness. While a semi-analytical algorithm exists for predicting spall and breach of RC slabs and non-load bearing walls, no comparable algorithm exists for spall and breach of RC columns. Because the early-time stress waves from a close-in detonation can reflect from both the back and side faces of a column, the column case is distinctly different from either the slab or the wall case.

As part of a broader effort by the United States Department of Homeland Security (DHS) to develop anti-terrorism planning tools, Protection Engineering Consultants (PEC) collaborated with the University of Texas at Austin (UT-Austin) and the US Army Engineer Research and Development Center (ERDC) to develop a fast-running model for predicting spall and breach of RC columns subjected to near-contact and contact detonations. Existing experimental data were supplemented with synthetic data developed from results of finite element models. The experimental and synthetic databases were used to define boundaries between regions of breach, spall, and no damage similar to the approach used in past research on slabs (Marchand and Plenge 1998 [1]). Points on the boundary between spall and breach were identified, and best-fit curves were applied to the boundary points. These best-fit curves define the baseline breach threshold. The Marchand and Plenge spall curve for bare charges was used as the baseline spall threshold curve. The baseline curves were plotted against available column spall/breach data and then modified to achieve agreement with the test data. The resulting factored curves were incorporated into a fast-running model for predicting breach, spall, and the extent of spall.

This work was funded by the DHS Science and Technology Directorate, Infrastructure Protection and Disaster Management Division. Permission to publish was granted by the Director, Geotechnical & Structures Laboratory.

INTRODUCTION

Protection Engineering Consultants (PEC), the University of Texas at Austin (UTA), and the US Army Engineer Research and Development Center (ERDC) collaborated to develop an anti-terrorism planning tool (ATP) that is a fast-running software for determining damage and failure of structural components due to terrorist attack.

In support of the ATP tool, PEC developed an algorithm for predicting spall and breach of a reinforced-concrete (RC) column. Spall refers to the loss of cross section through part of an element's thickness; breach refers to the loss of cross section through the entire thickness. These conditions are illustrated in Figure 1(a) and Figure 1(b), respectively. While a semi-analytical algorithm exists for predicting spall and breach of RC slabs and non-load bearing walls, no comparable algorithm exists for spall and breach of RC columns. Because the early-time stress waves in a column from a close-in detonation can reflect from both the back *and* side faces (2D shock propagation), the column case is distinctly different from the slab/wall case (1D shock propagation). This difference is illustrated by comparison of **Figure 2** and **Figure 3**.

In this paper, the development of threshold curves for predicting the damage state (breach, spall, or no damage) of a RC column is presented. The threshold curves were developed from a small set of empirical data and a large set of synthetic data using results from LS-DYNA® calculations.

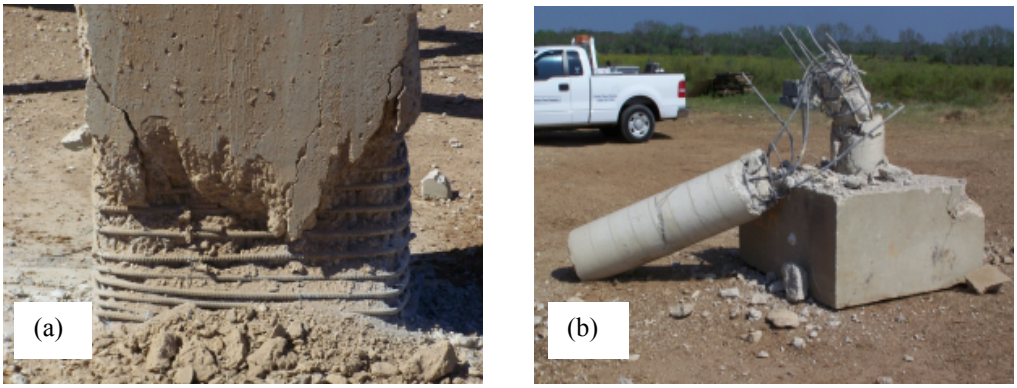

Figure 1. (a) Column Spall (b) Column Breach

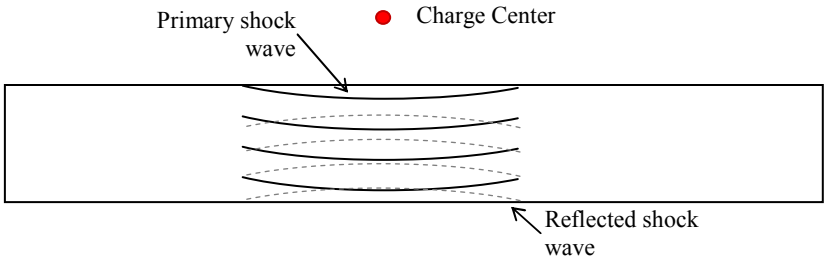

Figure 2. Slab or Wall: 1D Shock Propagation

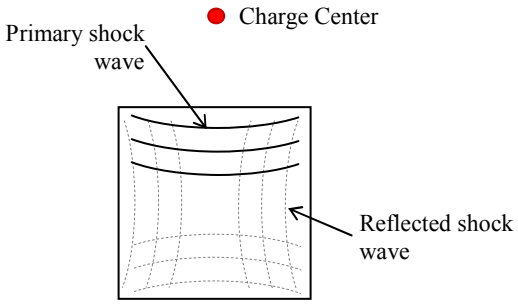

Figure 3. Column: 2D Shock Propagation

METHODOLOGY

The methodology discussed in AFRL-MN-EG-TR-1998-7032 *Concrete Hard Target Spall and Breach Model* [1], referred to hereafter as AFRL-98, was taken as the starting point for this effort. AFRL-98 details development of a spall/breach algorithm for RC slabs and walls. The AFRL-98 algorithm was based on a large database of empirical slab/wall tests. In contrast, empirical data for RC columns is sparse; available data consisted of 11 column tests performed as part of NCHRP 12-72, a test program supporting NCHRP Report 645 [2]. Therefore, development of the spall/breach algorithm for RC columns had two parts: (1) generation of synthetic data using LS-DYNA® and (2) representation of the synthetic and empirical data with a set of curves. The focus of this paper is the second part, description of damage state (breach, spall, or no damage) with a set of threshold curves. Additional discussion on the first part, generation of the synthetic data, can be found in Puryear et al. [3].

To briefly summarize, the synthetic data was inferred from results of 325 LS-DYNA computations of RC columns subjected to close-in and contact detonations. In those computations, the primary variables were the charge weight, standoff, column section type, and section dimensions. In all cases, the charge was cylindrical, and the *L/D* ratio was typically 1.0. Though generally held constant, the compressive strength of the concrete and longitudinal and transverse steel ratios were also varied. Column cross-sections were

- Circular
- Square
- Rectangular with $D/W = 2$
- Rectangular with $D/W = 0.5$

where D (depth) is the section dimension parallel to the standoff direction and W (width) is the section dimension perpendicular to standoff:

This synthetic data and limited empirical data were plotted in the τ vs. applied impulse plane of AFRL-98. τ is a measure of impulse attenuation through the target thickness. The applied specific impulse was calculated using the simplified equation in AFRL-98 that was modified to include clearing effects for the bounded concrete surface and a geometry reduction for the circular cross-section.

Points on the boundary between spall and breach were identified, and best-fit curves were applied to the boundary points. These best-fit curves defined the baseline breach threshold. The AFRL-98 curve for spall threshold (boundary between no damage and spall) for bare charges was used as the baseline spall threshold curve. The baseline curves were plotted against available column spall/breach data, and factors were applied to τ for agreement with the test data. The resulting factored curves were then implemented in ATP-B for prediction of the damage state for a given threat and column geometry.

THRESHOLD PARAMETERS

The AFRL-98 threshold curves are functions that relate applied impulse to τ. τ is qualitatively the inverse of an attenuation factor, which is based on target thickness, target elastic wave speed, applied specific impulse, and scaled standoff. Rate effects are included, and the strength increases as a function of load rate are based on work by Ross et al. [4].

As noted above, the AFRL-98 methodology was the starting point for this effort. The primary adjustment to that methodology was modifying the definition of target thickness (T). In the AFRL-98 methodology, T is simply the thickness of the RC slab or wall, as shown in Figure 4. The analogous parameter for a column would be its depth parallel to charge standoff. Defining T as the diameter for the circular column was found to be sufficiently accurate, but for the square and rectangular columns, T was defined as the distance from the center of the blastward face to the back corner. Definition of T is illustrated in Figure 5. This definition for the square and rectangular columns accounted for the effect of increased column width on the threshold and permitted the continuous transition from square to rectangular threshold curves.

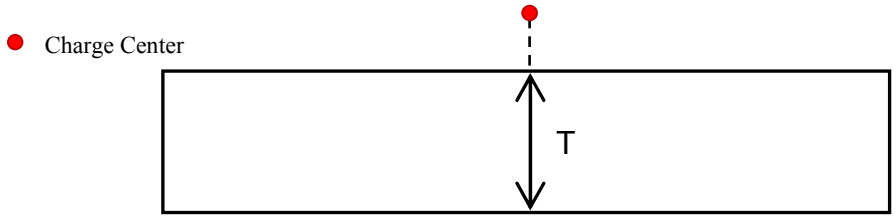

Figure 4. AFRL-98 Target Thickness

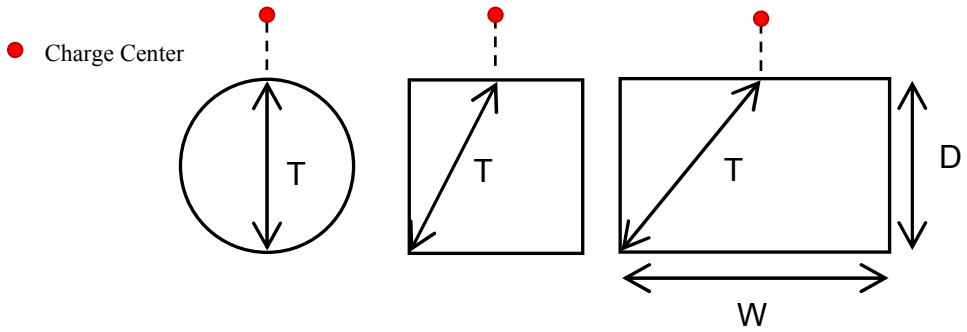

Figure 5. Effective Thickness of Target

APPLIED IMPULSE

The applied impulse was the peak specific applied impulse. It was calculated using Equation 13 in AFRL-98 at the point on the blastward target surface with normal through the center of the charge. AFRL-98 Equation 13 includes a charge weight and standoff term and was derived from Kingery-Bulmash relationships at very small standoff. Casing effects were neglected.

Prior to calculation of applied impulse, the charge weight was adjusted per AFRL-98 Equation 12. That equation assumes that the charge is cylindrical and parallel to the target face. Charge weight adjustment accordingly depends on cylinder height, cylinder diameter, initial charge weight, and standoff. The adjusted charge weight is then entered into AFRL-98 Equation 13, which is based on a spherical charge.

Two additional effects on applied impulse that are present for RC columns but not for RC slabs/walls are cross-section shape and clearing. Shape effects are due to the difference in how a circular cross section collects applied impulse compared to a square or rectangular cross section. Clearing is the influence of relief waves from free edges on applied impulse as a function of standoff from a limited width surface like a column.

Data and analytical procedures for both of these factors are sparse and limited for the loading regimes (small to moderate size explosive charges) and standoffs (close to near contact) considered for the RC column algorithm. Relevant data were generated for both factors during the performance of NCHRP 12-72 [2]. In a test series performed for the U.S. Army Engineer Research and Development Center (ERDC) [5], column shape effects on blast load were experimentally quantified through the performance of 8 tests of both square and circular cross-section columns ($1/8^{th}$ scale) and included the collection of 144 channels of blast pressure data. These data were evaluated and discussed in NCHRP Report 645 [2] and in Williams [5]. These data are considered separately from the clearing factor (dis-

cussed below) in that clearing was assumed to occur in the same way for both the square and circular columns considered in these tests. The results of that review suggested that a shape factor of approximately 0.75 is appropriate for columns of circular cross section as compared to equivalent-width square columns. This geometric effect is included before calculation of the adjusted charge weight.

The RC column algorithm also includes a clearing factor to take into account the edge effects that are present at moderate to larger standoffs. At the close standoffs considered by the algorithm, no known data are available to confirm the effect of clearing. However, the influence of clearing was determined by adjusting the clearing equation so that damage predicted by the algorithm corresponded with damage observed in NCHRP 12-72 [2]. The clearing equation follows the form of the understood airblast mechanics, i.e.,

- Near-contact and large effective presented areas result in no clearing effects.
- Clearing effects do become important for the range of close contact to larger standoffs where the width of the loaded element is similar to or larger than the standoff.

BASELINE CURVES

The threshold and applied impulse parameters were calculated for each of the 325 LS-DYNA results and 11 close-in column tests and plotted in the AFRL-98 τ vs. applied impulse plane. The damage states of the columns (breach, spall, or no damage) were distinguished by series in the τ vs. i_{app} plane. Boundary points defining the transition from the breach region to the spall region were identified, and best-fit curves applied to those points. In the plots, high-impulse and low-impulse regimes were evident. Consequently, close-in data (clear standoff greater than zero) and contact data were separated, and best-fit curves obtained for each. As a result, a close-in breach threshold curve and a contact breach threshold curve were developed for each section type. Examples of close-in and contact threshold curves for the circular section are shown in Figure 6 and Figure 7.

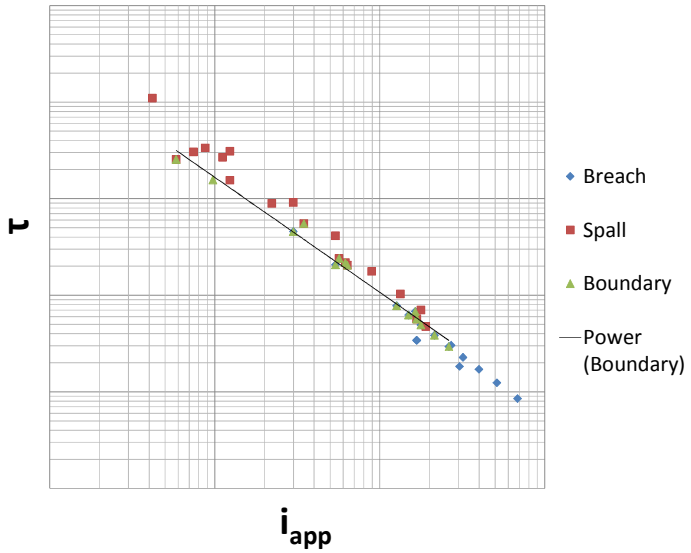

Figure 6. Breach Threshold for Close-in Detonation on Circular Column Section

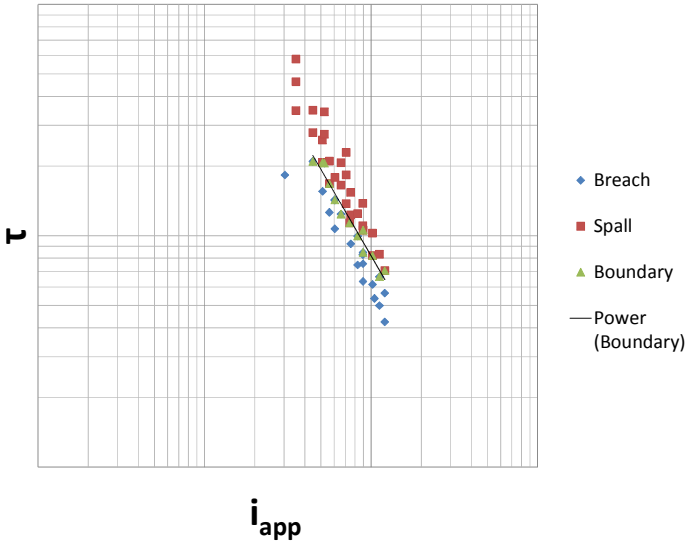

Figure 7. Breach Threshold for Contact Detonation on Circular Column Section

As shown in Figure 6 and Figure 7, the LS-DYNA data distinguished well between spall and breach for the highly energetic close-in and contact detonations. Because the difference between spall and no damage is small and defining this difference is subjective when analyzing the numerical results, the LS-DYNA modeling was less effective for distinguishing between spall and no damage. Therefore, the spall threshold curve (boundary between no damage and spall) for slabs from AFRL-98 was used as the baseline spall threshold curve for all column sections and factored as discussed below.

FACTORED CURVES

The baseline breach threshold curves were obtained from the LS-DYNA models, and the baseline spall threshold curve was obtained from AFRL-98. The curves were then factored to better match the available NCHRP 12-72 data (11 empirical data points). All breach threshold factors were less than 1. This is consistent with the observation that an LS-DYNA computation tends to over-represent damage. The LS-DYNA models provide an "x-ray" view of damage and likely identify damage not evident from posttest observations of an actual column specimen.

The NCHRP tests included eight circular cross sections, and these are shown in the τ-impulse plane with the factored curves in Figure 8. Seven data points are visible in Figure 8, because two of the tests were identical. The factored threshold curves divide the middle section of the plane into breach, spall, and no damage regions. The transition from the close-in to contact threshold curve is also noted.

For impulses less than the lower limit, there is no damage. For impulses greater than the upper limit, there is global rubblization, i.e., instead of sectional breach; much of the column is rubblized into high kinetic energy debris. The lower limit for impulse was selected based on the LS-DYNA results and NCHRP 12-72 data. The upper limit was defined by where the threshold curves intersect. In practice, it is difficult to reach such high impulses because, for a given geometry, as charge weight increases, the standoff distance to the center of the charge increases. Consequently, the applied impulse tends to plateau as the charge weight increases beyond a certain point.

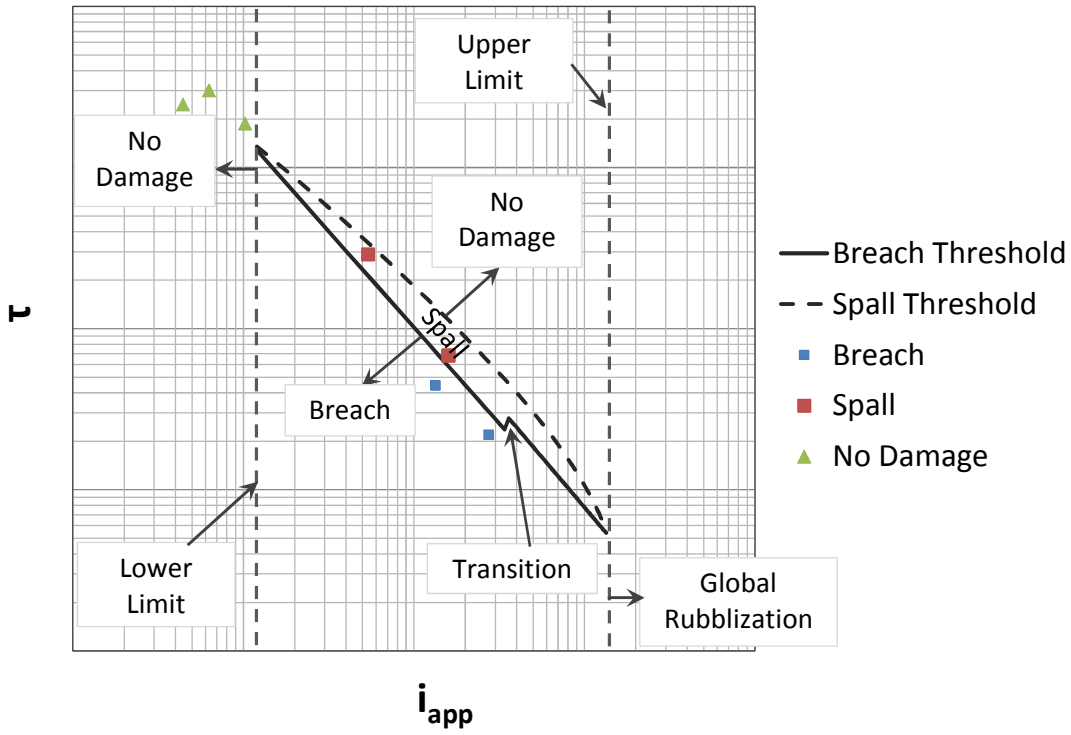

Figure 8. Factored Threshold Curves – Circular Cross Section

The process described above for the circular cross section was also followed for the square cross section. The only difference is that there were only 3 tests of square cross sections.

No rectangular cross-sections were tested in the NCHRP 12-72 program. Therefore, factors for the rectangular cross-sections were selected to provide a continuous transition from square cross-sections to rectangular cross-sections in both directions; i.e., factors were selected so that the damage state was the same over the transition from the square curves to the rectangular curves.

Depending on its aspect ratio, the threshold of a rectangular column would be calculated using threshold curves from either the square or rectangular computations. Therefore, transition ratios between the square and rectangular threshold curves were selected for implementation in the algorithm. Specifically, the transition ratio from the rectangular (D/W = 0.5) curve to the square curve (D/W = 1.0) is D/W = 0.75; the transition ratio from the square curve to the rectangular (D/W = 2.0) is D/W = 1.5. These transition D/W ratios and the threshold curves used in each interval are shown in Figure 9. As an example, if a rectangle has D/W less than 0.75, the threshold curves from the rectangular (D/W = 0.5) computations are used in the algorithm; if D/W is between 0.75 and 1.5, the threshold curves from square computations are used, etc.

The NCHRP 12-72 test data are compared to the algorithm in Table 1. In addition to reporting damage state, the algorithm reports the extent of spall damage on the side and rear of the column. No extent of damage is reported for breach cases, because empirical data were not available. Development of the curves for predicting spall damage is not discussed in this paper; however, spall damage reported by the algorithm for the NCHRP tests are included in Table 1 for completeness.

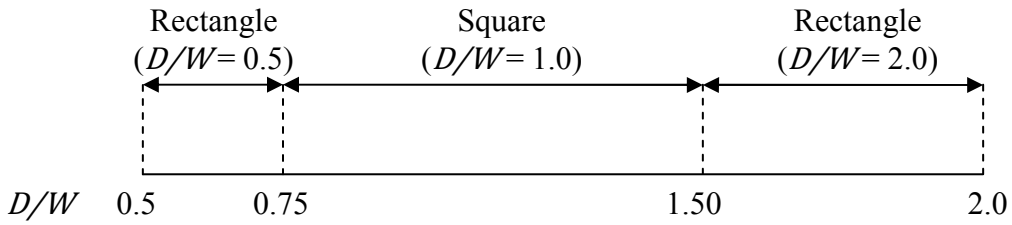

Figure 9. Transition Ratios for Square and Rectangular Threshold Curves

Table 1. Comparison of Algorithm Performance versus NCHRP 12-72 Tests

Test ID	NCHRP			Algorithm		
	Damage State	Side Damage in. (cm)	Rear Damage in. (cm)	Damage State	Side Damage in. (cm)	Rear Damage in. (cm)
BR1	Breach	na[1]	na[1]	Breach	na[1]	na[1]
BR3	Breach	na[1]	na[1]	Breach	na[1]	na[1]
BR2	Spall	60 (152)	48 (122)	Spall	61 (155)	36 (91)
BR4	Spall	60 (152)	48 (122)	Spall	61 (155)	36 (91)
BR5 (3A)	Spall	24 (61)	20 (51)	Spall	28 (71)	20 (51)
BR 5 (2-Blast)	Spall	30 (76)	0	Spall	24 (61)	16 (41)
3-Blast	Spall	30 (76)	20 (51)	Spall	49 (124)	18 (46)
3A	Spall	24 (61)	0	Spall	12 (30)	9 (23)

[1]No damage lengths reported for breach cases

CONCLUSIONS AND RECOMMENDATIONS

An algorithm for predicting damage state (breach, spall or no damage) of a RC column was described. The algorithm was based on a limited empirical data set and large synthetic data set. Recommendations for follow-on research are made below.

First, the current spall/breach algorithm accounts for an air burst of a cylindrical charge, which has a far-field spherical shock distribution. In the near field, the charge weight of cylinder is adjusted and assumed to propagate spherically. Insufficient data were available to include hemispherical shock distributions characteristic of a charge confined by a ground plane. Because a hemispherical configuration will likely apply energy differently to the target than a spherical configuration, the recommendation is that additional tests including hemispherical charge distributions be conducted.

Second, in all cases, the algorithm assumes a bare charge. Casing effects were not considered in the numerical modeling. Weapon fragments can significantly affect the extent of damage, and the recommendation is that their effects be examined in future research.

Third, the results of this spall and breach model could be used in the prediction of the residual capacity of a column damaged by close-in or contact detonations. For the threshold calculations, the effect of reinforcement configuration was expected to be negligible; the AFRL-98 the threshold parameter τ does not depend on reinforcement. However, the effect of transverse reinforcement and splices will likely be important to residual capacity. In general, concrete will spall or breach depending on the amount of material (thickness) that attenuates the shock. The amount of reinforcement has a minor, indirect effect on attenuation through the compressive strength of the concrete. In contrast, the reinforcement has a large effect on how much of the rubblized core remains intact, and the extent of intact core is a good indicator of residual capacity. Because a column segment with light transverse reinforcement or a longitudinal splice will have more difficulty keeping the core intact than a segment with heavy transverse or continuous longitudinal reinforcement, the column is expected to have significantly less residual capacity. Investigating the relationships among local damage, transverse reinforcement, state of the column core, and residual capacity should be researched.

ACKNOWLEDGEMENTS

This work was funded by the DHS Science and Technology Directorate, Infrastructure Protection and Disaster Management Division. The US Army Engineer Research and Development Center (ERDC) was program manager for this work. Permission to publish was granted by Director, Geotechnical and Structures Laboratory and is gratefully acknowledged.

REFERENCES

[1] K. A. Marchand and B. T. Plenge, "Concrete Hard Target Spall and Breach Model," AFRL-MN-EG-TR-1998-7032, Air Force Research Laboratory, March 1998.

[2] E. B. Williamson, O. Bayrak, G. D. Williams, C. E. Davis, K. A. Marchand, A. E. McKay, J. Kulicki, and W. Wassef, "NCHRP Report 645 Blast-Resistant Highway Bridges: Design and Detailing Guidelines," Transportation Research Board, National Cooperative Highway Research Program, Washington, D.C., 2010.

[3] J. M. H. Puryear, D. J. Stevens, K. A. Marchand, E. B. Williamson, and C. K. Crane, "ALE Modeling of Explosive Detonation on or near Reinforced-Concrete Column," in *12th International LS-DYNA Users Conference*, Dearborn, MI, 2012.

[4] C. Ross, S. Kuennen and J. Tedesco, "Effects of Strain-Rate on Concrete Strength," in *American Concrete Institute. Spring Meeting*, 1992.

[5] G. D. Williams, “Analysis and Response Mechanisms of Blast-Loaded Reinforced Concrete Columns,” University of Texas at Austin, May 2009.